Separation Science and Technology
Publication details, including instructions for authors and subscription information:
http://www.informaworld.com/smpp/title~content=t713708471

Comparison of Adsorption Dynamics in Kinetic and Equilibrium Beds in Hydrogen Ternary System

Min-Bae Kim[a]; Youn-Sang Bae[a]; Hyungwoong Ahn[a]; Chang-Ha Lee[a]
[a] Department of Chemical Engineering, Yonsei University, Seoul, Korea

Online publication date: 08 July 2010

To cite this Article Kim, Min-Bae , Bae, Youn-Sang , Ahn, Hyungwoong and Lee, Chang-Ha(2004) 'Comparison of Adsorption Dynamics in Kinetic and Equilibrium Beds in Hydrogen Ternary System', Separation Science and Technology, 39: 13, 2951 — 2976
To link to this Article: DOI: 10.1081/SS-200035947
URL: http://dx.doi.org/10.1081/SS-200035947

SEPARATION SCIENCE AND TECHNOLOGY
Vol. 39, No. 13, pp. 2951–2976, 2004

Comparison of Adsorption Dynamics in Kinetic and Equilibrium Beds in Hydrogen Ternary System

Min-Bae Kim, Youn-Sang Bae, Hyungwoong Ahn, and Chang-Ha Lee*

Department of Chemical Engineering, Yonsei University, Seoul, Korea

ABSTRACT

The adsorption dynamics of a ternary hydrogen mixture ($H_2/CH_4/CO$; 59.3/30.5/10.2 vol%) in a carbon molecular sieve (CMS) bed were compared experimentally and theoretically with fixed beds by using activated carbon, zeolite 5A, and oxidized CMS. The breakthrough experiments were performed in the range of 4–16 kg_f/cm^2 adsorption pressure and 4.5–9.1 LSTP (liter at standard temperature and pressure)/min feed flow rate. In the CMS bed regenerated at high temperature (548 K), the adsorption dynamics were similar to those in the activated carbon bed in terms of both breakthrough curves and temperature excursions due to the pore enlargement of the CMS regenerated at high temperature. Therefore, the effect of kinetic separation on the

*Correspondence: Chang-Ha Lee, Department of Chemical Engineering, Yonsei University, 134 Shinchon-dong, Sudaemun-gu, Seoul 120-749, Korea; Fax: +82-2-312-6401; E-mail: leech@yonsei.ac.kr.

DOI: 10.1081/SS-200035947 0149-6395 (Print); 1520-5754 (Online)

adsorption dynamics was not observed. However, in the CMS bed regenerated at low temperature (423 K), CH_4 showed a breakthrough earlier than CO, owing to the sieving effects on the CMS, and CO showed the wide mass transfer zone. To understand the adsorption characteristics and the thermal effects by the heat of adsorption, a nonisothermal dynamic model incorporating mass, energy, and momentum balances was applied to the adsorption dynamics in the kinetic and equilibrium separation beds. Moreover, the kinetic effects on the adsorption dynamics also were studied by using a constant or variable diffusivity model.

Key Words: Adsorption dynamics; Ternary hydrogen mixture; CMS; Kinetic effect; Thermal effect.

INTRODUCTION

The fixed-bed adsorption process, especially pressure swing adsorption (PSA), has been an important unit operation for purification and bulk separation of gas mixture. In recent years, the PSA process has been commercialized increasingly for air-drying, hydrogen purification, air separation, and various other separations.[1,2] One of the successful applications of the PSA process is hydrogen recovery, because a high-purity H_2 product with high productivity can be obtained from a well-designed PSA.

Separation of a gas mixture by PSA generally is accomplished by either selective adsorption (equilibrium separation) or by differences in the diffusion rates of different molecules into an adsorbent (kinetic separation). A third mechanism (steric separation) derives from the molecular sieving property of zeolite. Carbon molecular sieve (CMS) has a bidispersed pore structure with clearly distinguishable macropores and micropores, and its micropore size is known in the range of 3–5 Å.[3] This adsorbent has the pores of molecular dimensions that provide relatively high adsorption capacity and kinetic selectivity for various gases.[4] The typical kinetic separation process that is commercialized is air separation, which produces nitrogen and uses CMS as an adsorbent. Recently, kinetic separation of methane/carbon dioxide and recovery of carbon dioxide from landfill gas has been studied.[5,6] In spite of such potential capacities of kinetic separation, it is mainly because little is understood about it that there have only been few commercial applications of it up to now.

The adsorption dynamics for a fixed-bed bulk component system has been studied extensively.[7–11] In a multicomponent mixture, the breakthrough behavior generally includes a roll-up or plateau phenomenon and temperature variation in the bed. Farooq and Ruthven[12] pointed out that roll-up can take

place in an equilibrium control system as well as in a kinetically controlled system. Moreover, it is suggested that multiple roll-ups in the equilibrium separation system could be stemmed not only from different equilibrium affinity but also from sorption kinetics.[13] Recently, Ahn et al.[14] compared the adsorption thermal effects on the roll-up between an activated carbon bed and a zeolite 5A bed. In the case of a CMS bed, Gupta and Farooq[15] reported that the deviation between PSA simulation and experimental data appeared to increase with increasing operating pressure in the air separation PSA on CMS, because diffusivity has stronger dependence on surface coverage at wide pressure range.

The experimental results in the fixed bed for such useful information as breakthrough time, adsorption dynamics, and the amount of heat release can be used to develop a novel PSA process. In this study, the adsorption dynamics of the CMS bed were compared with those of the other beds packed with activated carbon and zeolite 5A through breakthrough experiments by using a ternary hydrogen mixture ($H_2/CH_4/CO$). Moreover, the change of the kinetic separation efficiency in the CMS bed was studied by using the CMS bed regenerated at different temperature because the change of pore size distribution, caused by regenerating the adsorbents at different temperatures and surrounding conditions, can affect the adsorption dynamics, especially in a kinetically controlled system. A nonisothermal dynamic model incorporating mass, energy, and momentum balances was applied for the experimental results by using the gPROMS modeling tool.[16] In addition, the effect of diffusional time constants on the adsorption dynamics was studied by using several rate models with a constant or a variable diffusivity. Since temperature variation during the adsorption process is inevitable, the adsorption dynamics and roll-up phenomenon in each bed were investigated according to the relationship between the concentration and the temperature profiles.

EXPERIMENTAL

The schematic diagram of an experimental apparatus is shown in Fig. 1. The adsorption bed was made of stainless steel of 100-cm length and 3.71 cm ID. Four resistance temperature detectors (Pt 100 Ω) were installed at the position of 10, 30, 50, and 75 cm from the feed end to probe the temperature variation inside the bed, and two pressure transducers were located at the feed and product ends to measure the pressure variation. The precalibrated mass flow controller (Bronkhorst High-tech, F-201C, Ruurlo, The Netherlands) was installed between the feed tank and the adsorption bed to control the feed flow rate. The total amount of gas was confirmed by a wet gas meter (Shinagawa, W-NK-1B, Tokyo, Japan). The electrical back-pressure

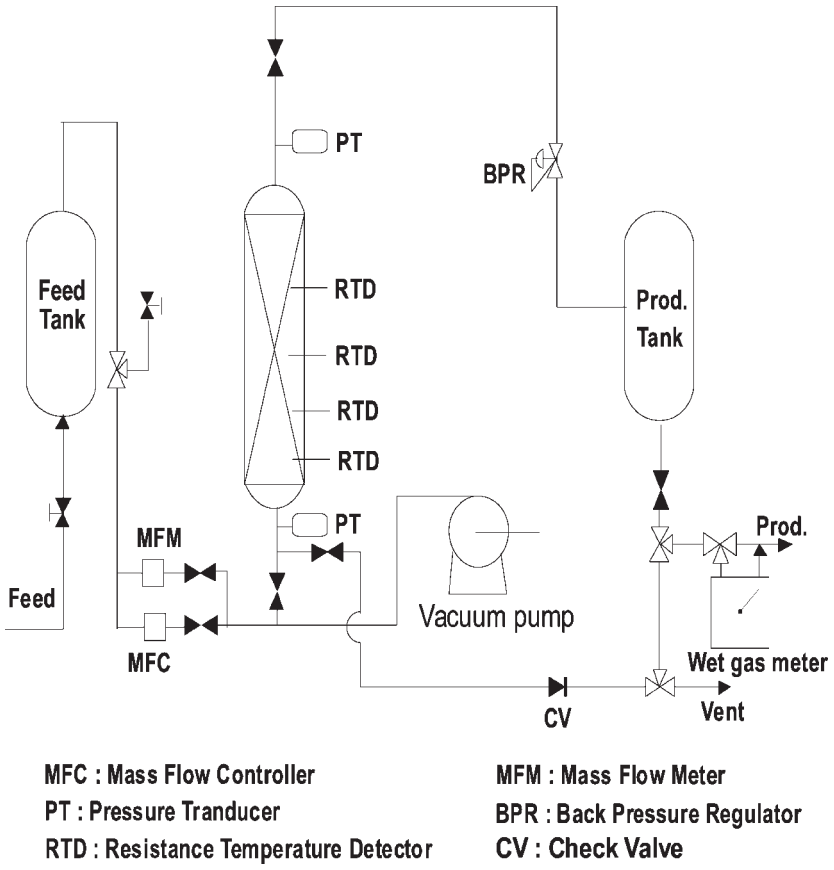

Figure 1. Schematic diagram of apparatus for breakthrough experiments.

regulator (Bronkhorst High-tech, P-702C, Ruurlo, The Netherlands) between the adsorption bed and the product tank was installed to maintain constant adsorption pressure in the bed. Effluent stream was sampled between the back-pressure regulator and the product tank and was analyzed by using a mass spectrometer (Balzers, QME 200, Liechtenstein, Germany). All the data, including concentration, temperature, pressure, and flow rate, were saved on the computer. Details of the equipment and the operating procedures used are described in the previous work.[17]

The hydrogen ternary mixture ($H_2/CH_4/CO$; 59.3/30.5/10.2 vol%), which is a main composition in the coke gas, was used as feed gas and the CMS (CMS-3A, Takeda Co., Osaka, Japan) as an adsorbent in a breakthrough

experiment. Prior to each experiment, the CMS was regenerated for 12 hr at 423 K in the vacuum condition and 548 K in the air condition. Then the bed packed with the CMS was vacuumed at 10^{-5} Torr.

The breakthrough experiments were performed in 4.5, 6.8, and 9.1 LSTP/min feed flow rate and 4, 10, and 16 kg_f/cm^2 adsorption pressure. And the adsorption bed was saturated initially with H_2 at the adsorption pressure.

MATHEMATICAL MODELS AND SIMULATION

To understand the dynamic behaviors of the CMS bed, the mathematical models were developed on the basis of the following assumptions: (i) the gas phase behaves as an ideal gas mixture, (ii) radial concentration and temperature gradients are negligible, (iii) thermal equilibrium between adsorbents and bulk flow is assumed, (iv) the flow pattern is described by the axially dispersed plug flow model, and (v) the pressure drop along the bed is considered by using the Ergun's equation. The assumption of neglecting radial gradient was accepted widely by numerous studies, and the others are also common assumptions in simulating the adsorption processes.[12–14,17–19]

The component and overall mass balance for the bulk phase in the adsorption bed are given by

$$-D_L\frac{\partial^2 c_i}{\partial z^2}+\frac{\partial(uc_i)}{\partial z}+\frac{\partial c_i}{\partial t}+\rho_p\left(\frac{1-\varepsilon}{\varepsilon}\right)\frac{\partial\overline{q_i}}{\partial t}=0 \tag{1}$$

$$\frac{\partial C}{\partial t}+\frac{\partial(uC)}{\partial z}+\frac{1-\varepsilon}{\varepsilon}\rho_p\sum_{i=1}^{n}\frac{\partial\overline{q_i}}{\partial t}=0 \tag{2}$$

where D_L is an axial dispersion coefficient calculated from the Wakao correlation[1,11] and second-order concentration gradient is negligible in the overall mass balance.

Another characteristic of the adsorption process is the temperature variation caused by the heat of adsorption. In this system, the energy balance for the gas phase also includes the heat transfer to the column wall:

$$-K_L\frac{\partial^2 T}{\partial z^2}+(\varepsilon_t\rho_g C_{pg}+\rho_B C_{ps})\frac{\partial T}{\partial t}+\varepsilon\rho_g C_{pg}\frac{\partial(uT)}{\partial z}$$
$$-\rho_B\sum_{i=1}^{n}(-\overline{H_i})\frac{\partial\overline{q_i}}{\partial t}+\frac{2h_i}{R_{Bi}}(T-T_w)=0 \tag{3}$$

where K_L is the effective axial thermal conductivity.

To consider heat loss through a wall and heat accumulation in the wall, another energy balance for the wall of the adsorption bed was used:

$$\rho_w C_{pw} A_w \frac{\partial T_w}{\partial t} = 2\pi R_{Bi} h_i (T - T_w) - 2\pi R_{Bo} h_o (T_w - T_{atm}) \tag{4}$$

where $A_w = \pi(R_{Bo}^2 - R_{Bi}^2)$.

The boundary conditions of mass and energy balances are presented below. The well-known Danckwarts boundary conditions were applied:

$$-D_L \left(\frac{\partial c_i}{\partial z}\right)\bigg|_{z=0} = u|_{z=0}(c_i|_{z=0^-} - c_i|_{z=0^+}); \quad \left(\frac{\partial c_i}{\partial z}\right)\bigg|_{z=L} = 0 \tag{5}$$

$$-K_L \left(\frac{\partial T}{\partial z}\right)\bigg|_{z=0} = \rho_g C_{pg} u|_{z=0}(T|_{z=0^-} - T|_{z=0^+}); \quad \left(\frac{\partial T}{\partial z}\right)\bigg|_{z=L} = 0 \tag{6}$$

where $c_i|_{z=0-}$ means feed concentration for component i.

To consider the pressure drop along the bed, Ergun's equation was introduced as momentum balance.[20,21]

$$-\frac{dP}{dz} = a\mu v + b\rho v|v| \tag{7a}$$

$$a = \frac{150}{4R_P^2}\left(\frac{1-\varepsilon}{\varepsilon}\right)^2, \quad b = \frac{1.75}{2R_P}\left(\frac{1-\varepsilon}{\varepsilon}\right) \tag{7b}$$

where v is superficial velocity.

The measurement of mixed-gas adsorption becomes more difficult as the number of component in the mixture increases. From pure gas isotherms for each constituent in the mixture, the adsorption equilibrium of multicomponent was described by the following extended Langmuir–Freundlich model:

$$q_i^* = \frac{q_{mi} B_i P_i^{n_i}}{1 + \sum_{j=1}^{n} B_j P_j^{n_j}} \tag{8a}$$

$$q_m = k_1 + k_2 T, \quad B = k_3 e^{k_4/T}, \quad n = k_5 + \frac{k_6}{T} \tag{8b}$$

This correlation has been used widely for the simulation and design of adsorbers and the cyclic gas separation processes because of its mathematical simplicity and extensibility to multicomponents.[1,2,4,14]

It is well known that the sorption rate in the kinetically controlled PSA process strongly depends on the concentration.[1,2,22,23] In this study, the following three sorption models were applied to investigate the kinetic effect on the adsorption dynamics: linear driving force (LDF) model with constant diffusivity, Darken's relation, and structural diffusion model.[4]

However, there are only few theories with which one can predict multi-component diffusivities from pure-component diffusivities, despite the importance of description of multicomponent diffusion inside porous material.[3] Among others, the Maxwell–Stefan theory yields alternative approaches to multi-component diffusion and is consistent with the theory of irreversible thermodynamics.[24–26]

Since the driving force for mass transport by diffusion is a chemical potential gradient in this theory, this driving force is balanced by the friction between the diffusing species and the pore wall. By comparing the driving forces for diffusion given by Fick's law and the Maxwell–Stefan equations, the following explicit expression for [D] can be obtained.

$$[D] = [B]^{-1}[\Gamma] \tag{9}$$

For the single file diffusion mechanism, the above equations simply give the following expressions for the Fick diffusivity matrix [D]:

$$[D] = \begin{bmatrix} \mathcal{D}_1 & 0 & 0 & 0 \\ 0 & \mathcal{D}_2 & 0 & 0 \\ 0 & 0 & \ddots & 0 \\ 0 & 0 & 0 & \mathcal{D}_n \end{bmatrix} [\Gamma] \tag{10}$$

The thermodynamic factor Γ is given by

$$\Gamma_{ij} = \theta_i \frac{\partial \ln p_i}{\partial \theta_j}, \quad i, j = 1, 2, \ldots, n \tag{11}$$

For Langmuir–Freundlich isotherm Γ is

$$\Gamma_{ij} = \frac{1}{n_i}\left(\delta_{ij} + \frac{\theta_i}{\theta_V}\right), \quad i, j = 1, 2, \ldots, n \tag{12}$$

As a result, the Fick diffusivity matrix [D] for ternary mixtures can be obtained as follows:

$$[D] = \frac{\begin{bmatrix} \mathcal{D}_1 & 0 & 0 \\ 0 & \mathcal{D}_2 & 0 \\ 0 & 0 & \mathcal{D}_3 \end{bmatrix} \begin{bmatrix} (1-\theta_2-\theta_3)/n_1 & \theta_1/n_1 & \theta_1/n_1 \\ \theta_2/n_2 & (1-\theta_1-\theta_3)/n_2 & \theta_2/n_2 \\ \theta_3/n_3 & \theta_3/n_3 & (1-\theta_1-\theta_2)/n_3 \end{bmatrix}}{(1-\theta_1-\theta_2-\theta_3)} \tag{13}$$

Model I: LDF Model with Constant Diffusivity

$$\frac{\partial \overline{q_i}}{\partial t} = \omega_i\left(q_i^* - \overline{q_i}\right), \quad \omega_i = \frac{KD_{ei}}{r_c^2} \tag{14}$$

In this model, with a single lumped mass transfer parameter, the effective diffusivity, D_{ei}, was assumed constant and was obtained from the mean value in the range of partial pressure of each gas.[4,27]

Model II: Darken Model with L–F Isotherm

Farooq et al. introduced a variable diffusivity model to a kinetically controlled PSA separation process. They pointed out that the Darken equation [Eq. (15)] with the Langmuir isotherms predicted the experimental data better than the constant diffusivity assumption. Based on those results, the following variable diffusivity models [Eq. (16)] were presented as the adsorption rate models.[1,23]

$$D_{ei} = D_{oi}\frac{d\ln P_i}{d\ln q_i} \tag{15}$$

$$D_{ei} = \frac{D_{oi}}{n_i}[1 + B_i P_i^{ni}] \tag{16}$$

which is reduced to constant diffusivity at low loading, as required.

It is noteworthy that the same resultant expression, Eq. (16), can be derived from the Maxwell–Stefan model for the single file diffusion mechanism in Eq. (13).

Model III: Structural Diffusion Model with L–F Isotherm

However, it was reported that the validity of substituting the activity of the adsorbed molecules by the gas-phase pressure in Darken's relation is not clear.[2] Recently, Do[28] proposed a structural diffusion model [Eq. (17)], derived from the assumption that the gradient of the isotherm is large. Based on those results, the following model [Eq. (18)] was proposed.

$$D_{ei} \approx \frac{D_{oi}}{dq_i/dP_i} \tag{17}$$

$$D_{ei} = D_{oi}\frac{(1 + B_i P_i^{n_i})^2}{P^{n_i - 1}} \tag{18}$$

The adsorption isotherms and LDF kinetic parameters for each pure gas on zeolite 5A and activated carbon were obtained from the previous work.[17] Models II and III depict the adsorption rate as a function of the adsorbate concentration of a solid phase. The adsorption isotherm and kinetic parameters on the CMS used in this study have been taken from independent single-component experiments by using a volumetric method.[4,29] Figure 2 shows the adsorption isotherms of three pure gases on the CMS with the corresponding regeneration conditions. The isotherm parameters and apparent time constant at zero pressure are summarized in Tables 1 and 2.

The numerical solution of the above model is very complex and is difficult, because the equations to determine the behavior of this system are what are called partial differential-algebraic equations (PDAEs). Furthermore, the exponential terms of non-linear isotherms (extended Langmuir–Freundlich model) and the variable adsorption rate with pressure often make numerical

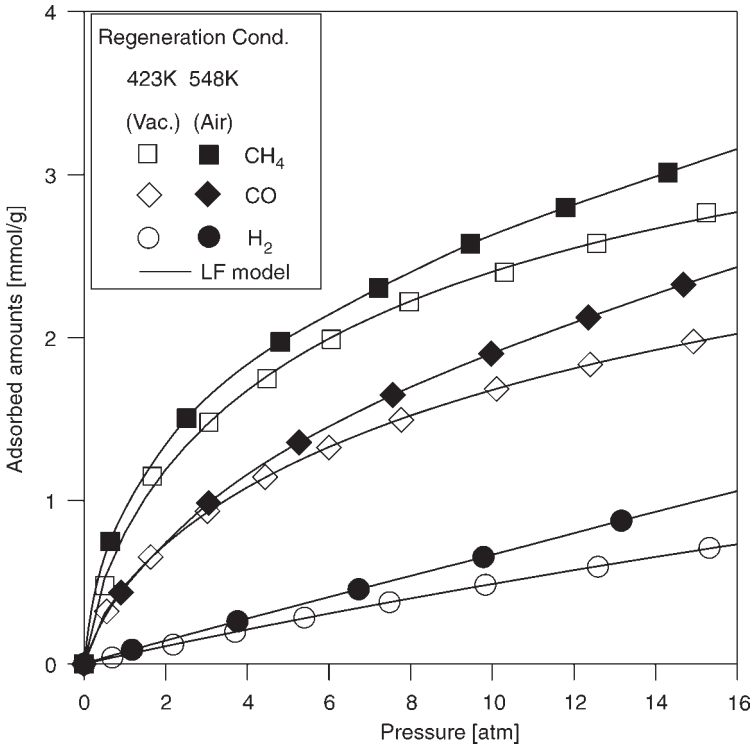

Figure 2. Adsorption isotherms of three pure gases (CH_4, CO, and H_2) at 293 K on CMS regenerated at different temperature.

Table 1. Parameter values of Langmuir–Freundlich model at 293 K.

	Regenerated at 423 K			Regenerated at 548 K		
	q_m (mmol/g)	B (1/atm)	n (—)	q_m (mmol/g)	B (1/atm)	n (—)
CO	4.18	0.130	0.714	10.25	0.050	0.660
CH_4	4.59	0.232	0.671	10.86	0.097	0.518
H_2	4.48	0.013	0.990	11.35	0.006	0.104

simulation inexecutable. In this study, the gPROMS modeling tool developed by Process Systems Enterprise Ltd. (London, UK) was used to obtain the solution of dynamic simulation from the above model. The systems of PDAEs are solved by using a method of line methodology, which uses the discrete-spatial dimension to reduce the PDAEs to differential-algebraic equations (DAEs). Typically, 100 distance steps were used for normal computation. A centered finite difference method of the second-order was applied to the spatial partial derivatives. And thereafter, the DAEs for temporal domain were integrated by using an integrator, called a DASOLV, included in the gPROMS library. The results of numerical simulation were stable for the range of conditions used in this work.

The central processing unit (CPU) time for solving the above PDAEs was less than 100 sec on a computer (PC; pentium 1.0 GHz), whereas each experimental run was executed for 1600 sec.

RESULTS AND DISCUSSION

Comparison of Adsorption Dynamics at Various Fixed Beds

Figure 3 shows the experimental and simulated breakthrough curves under the condition of 10 kg_f/cm^2 adsorption pressure and 6.8 LSTP/min feed flow rate at four different beds. The CMS used in Fig. 3a and d was

Table 2. Apparent time constant at zero pressure, D_{oi} (sec^{-1}) at 293 K.

	Model II: Darken model with L–F isotherm	Model III: Structural diffusion model with L–F isotherm
CO	0.0014	0.0076
CH_4	0.000011	0.0000031

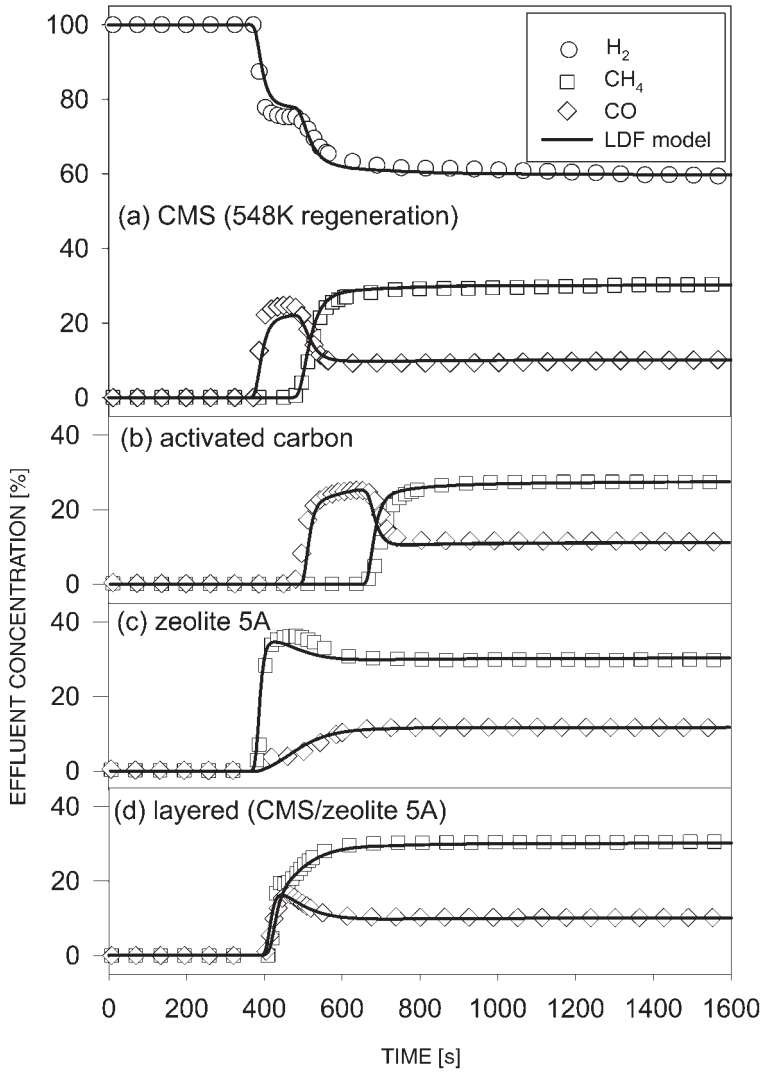

Figure 3. Breakthrough curves in (a) CMS (regenerated at 548 K), (b) activated carbon, (c) zeolite 5A, and (d) layered (CMS/zeolite 5A) bed under 10 kg_f/cm^2 adsorption pressure and 6.8 LSTP/min feed rate.

regenerated at 548 K. And the layered bed was packed with CMS and zeolite 5A in a 50 : 50 volume ratio. In this study, hydrogen was considered not an inert gas, but an adsorbate, although the isotherm amount of H_2 was much lower than that of CH_4 and CO. Therefore, the equilibrium as well as kinetic parameters of hydrogen on each CMS were taken into account in Eqs. (8) and (14). Since the H_2 breakthrough curve was balanced exactly with the amount of CH_4 and CO as shown in Fig. 3a, it was not presented in other figures to compare simultaneously the results of adsorption dynamics at various beds.

It is expected that two concentration wave fronts move along the adsorption bed with its propagation velocity in the equilibrium separation system. The velocity of each concentration wave front of CH_4 and CO can be determined mainly by feed rates, feed compositions, and adsorption capacities. Also, the equilibrium or kinetic relationship between the adsorbed species can change it. In the CMS bed regenerated at 548 K in Fig. 3a, the roll-up of CO is due to different equilibrium affinity between CO and CH_4 on the CMS as shown in Fig. 2. The overall behavior in the CMS bed resembles that of the activated carbon bed in Fig. 3b. However, compared with the behaviors in the activated carbon bed, the breakthrough time of each component and the interval between breakthrough times of CO and CH_4 were shorter and the roll-up of CO in the CMS bed became smaller and narrower. On the other hand, in case of the zeolite 5A bed in Fig. 3c, CH_4 was the first breakthrough component followed by CO at short intervals. Since both wave fronts of CH_4 and CO proceeded almost simultaneously, only relatively small roll-up of CH_4 was observed. Figure 3d shows the breakthrough curves of a CMS/zeolite 5A layered bed. The first breakthrough component was CO but CH_4 also made a breakthrough almost simultaneously. The wave front of CO was very sharp and fast in the CMS bed as shown in Fig. 3a and it became rather smooth and slow as it penetrated into the zeolite layer. The breakthrough times of both CO and CH_4 were between those of CMS bed and zeolite bed.

It is very interesting that CH_4 in the CMS bed shows relatively smooth wave front even though the isotherm on the CMS is favorable. However, the wave front of CO in this bed was sharp, which was similar to that in the activated carbon bed. In an equilibrium model, which assumes negligible resistance to mass transfer, it is reported that high-concentration fronts propagate faster than low-concentration fronts for a favorable isotherm. Thus, the concentration front is of self-sharpening type, referred to as a compressive wave.[2] But this model does not recognize the kinetic contribution to the formation of concentration gradients within the adsorbent. Therefore, the shape of CH_4 breakthrough curve became rather sagged owing to diffusional resistance into micropore of the CMS. So regardless of the dominant mechanism, the other effects should be considered.

It is reported that the diffusion rate of CH_4 was much slower than that of CO in the CMS with the average pore size of 3Å due to the tetrahedral molecular structure of CH_4.[4,5] However, the beds packed with the CMS regenerated at 548 K did not show any salient difference in the adsorption dynamics, compared with the equilibrium separation beds such as zeolite 5A and activated carbon beds. Moreover, when Model I (LDF model with constant diffusivity) was applied in these four experiments as an adsorption rate model, the predicted results agree well with the experimental breakthrough curves.

In this study, the variation of the adsorption dynamics by the CMS regenerated at the different temperature conditions was investigated because this temperature changed the adsorption characteristics of the CMS.

Effects of Regeneration Temperature on Adsorption Dynamics in the CMS Bed

Figure 2 also shows the adsorption isotherms on the CMS regenerated at 423 K under the vacuum condition. In terms of selectivity, both CMSs show small difference, while the adsorption capacity of the CMS activated at 548 K was higher than that of the other CMS. Furthermore, it was found from the BET (Brunauer, Emmett and Teller) analysis that the pore size of the CMS activated at 548 K under the air condition was enlarged at the average pore size of 4Å and its surface area was 522.59 m^2/g. At the experimental condition used in the work, the mean value of diffusion constant (D_e/R_p^2) of CO on the CMS regenerated at 423 K was about 1.2×10^2 times higher than that of CH_4.[30] However, in the case of CMS regenerated at 548 K, the ratio was less than an order of magnitude. Kinetic separation is possible only with molecular sieve carbon, because the distribution of pore size allows different gases to diffuse at different rates while totally avoiding exclusion of any gases in the mixture.[2] As a result, since the CMS used in Fig. 3a and d was regenerated at 548 K under the air condition, the kinetic effect became weak in the adsorption dynamics, while the equilibrium separation contributed much to the breakthrough curve.

The comparison of the breakthrough curves at the CMS beds regenerated at two different temperatures is presented in Fig. 4. This figure shows the dimensionless effluent concentration of CH_4 and CO under the same condition as that in Fig. 3. And the breakthrough results in each CMS bed were compared with the simulated ones with various adsorption rate models.

As can be seen in Fig. 4a, there is little contrast between simulated results when using three different rate models in the CMS regenerated at 548 K and the roll-up is mainly due to different equilibrium affinity between CO and

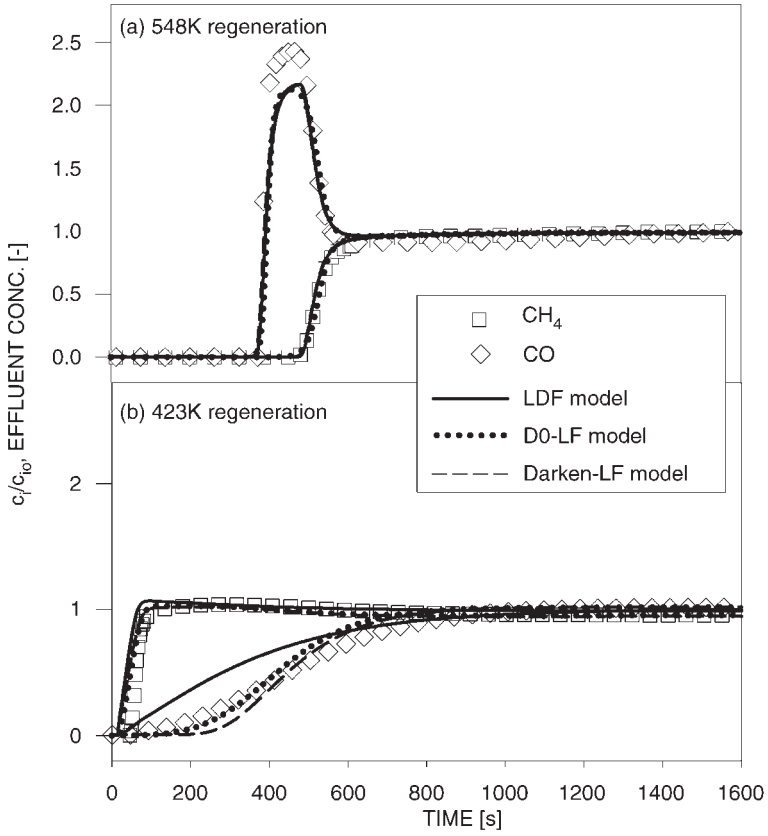

Figure 4. Experimental and simulated breakthrough curves in each CMS bed, regenerated at 548 and 423 K, under 10 kg_f/cm^2 adsorption pressure and 6.8 LSTP/min feed rate.

CH_4 on the CMS as mentioned above. This figure exhibits the typical roll-up features for the conventional equilibrium operations.

However, in the CMS bed regenerated at 423 K, the breakthrough order of the components is interchanged, caused by the kinetic effect. Moreover, the breakthrough of a heavy component occurred almost immediately due to the much slower uptake of CH_4. Compared with Fig. 4a, the breakthrough time of the light component, CO, was faster and the steepness of its breakthrough curve was reduced more saliently. Then, the convergence time into feed concentration was longer in Fig. 4b than in Fig. 4a. The equilibrium adsorbed amounts of CO on the CMS regenerated at 423 K are slightly

less than those at 548 K in the range of partial pressure, as shown in Fig. 2. These phenomena resulted from slower diffusion rate of CO on the CMS regenerated at 423 K. It means that the contact time is too short to permit significant uptake of a light component in the pore of the CMS. In other words, the concentration wave front could be controlled by the control of the pore size on CMS.

It is noteworthy that the slight roll-up of a heavy component, CH_4, is observed in Fig. 4b. This phenomenon was not seen in equilibrium CMS operation in Fig. 4a. CH_4 on the CMS showed the most favorable isotherm in the system in Fig. 2, and its concentration in the feed was higher than CO. However, the result in Fig. 4b implies that the CO concentration in the pore of the CMS is higher than CH_4 concentration due to the faster diffusion rate of CO than that of CH_4. And, it is clear that the adsorption dynamics in this bed totally depends on the kinetic effect.

As appeared in Fig. 4a, there is no difference among the predicted results in three different rate models. However, Models II and III (variable diffusivity models) predicted the experimental data much better than Model I (constant diffusivity model) in the case of the kinetic separation bed in Fig. 4b. Since the experiments were performed at a low pressure range in terms of partial pressure of CO and CH_4, there was only a negligible difference between the predicted results in the structural diffusion model (Model III) and the Darken's model (Model II).

The effects of adsorption pressure on breakthrough curve in each CMS bed are presented in Figs. 5 and 6. In Fig. 5, since the difference in the adsorption capacities of CO and CH_4 on the CMS became greater with an increase in the adsorption pressure, these two concentration wave fronts were separated further apart and the roll-up of CO by CH_4 was increased. The adsorption dynamics in the bed due to the change in the adsorption pressure were similar to those in the activated carbon bed[14] because selective adsorption plays a more important role in the adsorption operation than the difference in the diffusion rates of molecules.

Figure 6 shows that in the CMS bed regenerated at 423 K, the breakthrough time of CH_4 is increased as the adsorption pressure is increased. The higher the pressure of each component, the faster they diffuse. It implies that the diffusion rates of both components depend on the adsorption pressure. However, the elongation of the CH_4 breakthrough time within this pressure range in the kinetic bed was much smaller than that in the equilibrium bed in Fig. 5. Moreover, the breakthrough curve of CO became smoother with an increase in the adsorption pressure because the adsorption amount of a stronger adsorbate, CH_4, was increased with pressure.

To understand the dynamic behavior clearly, bed concentration profiles at different times are illustrated in Figs. 7 and 8. These figures show the

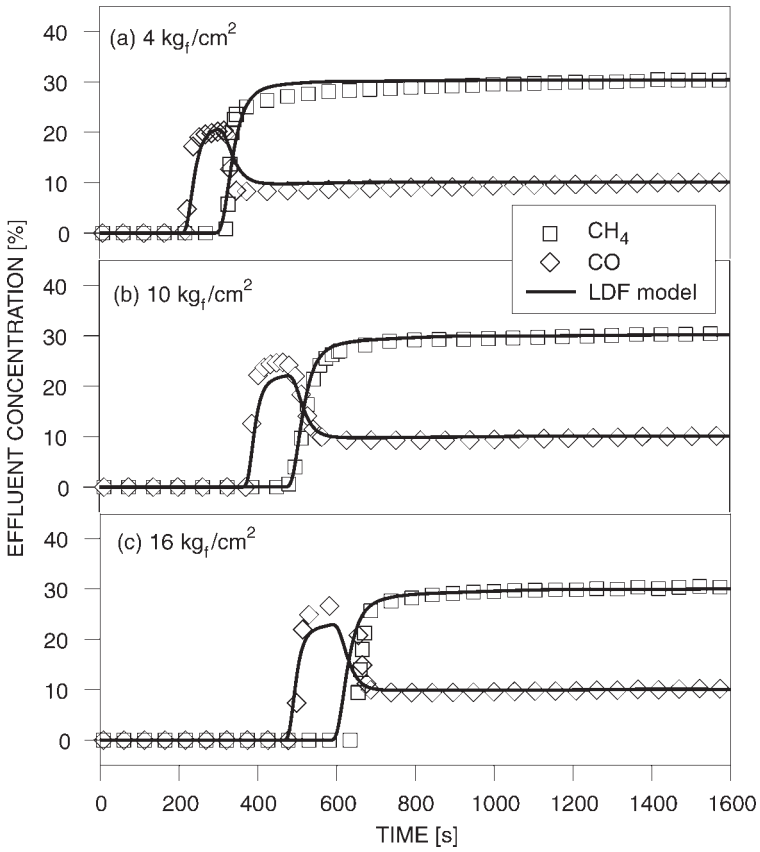

Figure 5. Effect of adsorption pressure on breakthrough curves at constant 6.8 LSTP/min feed rate in the CMS bed regenerated at 548 K.

gas-phase mole fraction and dimensionless loading of each component as a function of dimensionless bed length. Since q^* is a function of temperature and partial pressure, it is not constant but variable (i.e., q^* is also a function of both length and time). In an equilibrium control system, as shown in Fig. 7, the concentration wave front of a light component propagates faster than that of a heavy component. The roll-up of CO in Fig. 7b results from the fact that light components lose their adsorption sites due to the competitive adsorption of heavier components. Therefore, the desorbed light components join the bulk stream and the gas-phase concentration becomes greater than that in the feed concentration. It is notable that $\bar{q}$ also exceeds q^* for CO in the early region of a roll-up. Figure 7c shows that the system at that time is in

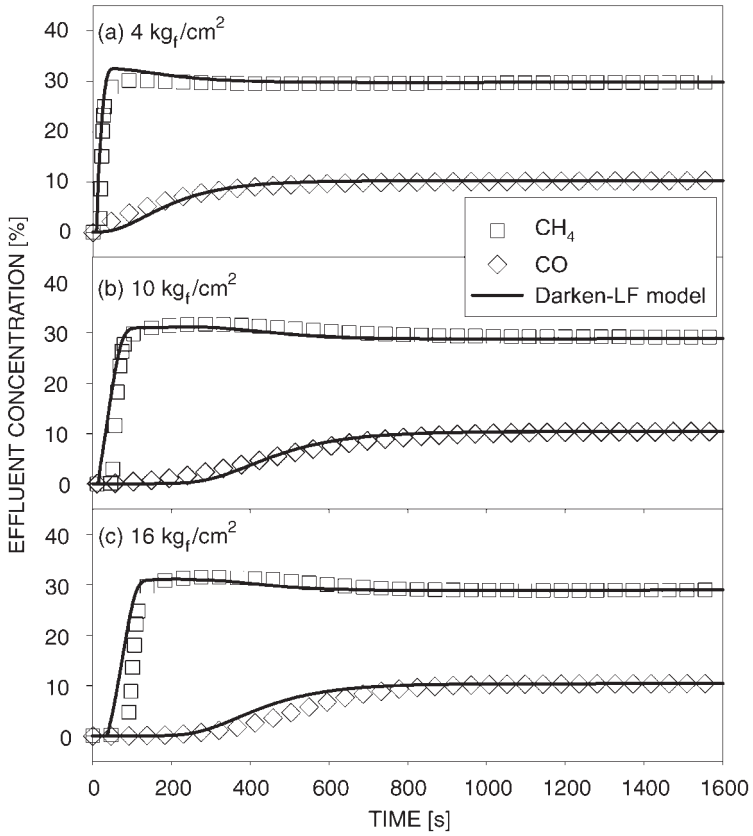

Figure 6. Effect of adsorption pressure on breakthrough curves at constant 6.8 LSTP/min feed rate in the CMS bed regenerated at 423 K.

equilibrium, because there is no driving force of mass transfer between the gas and the solid phases.

In a kinetically controlled system such as Fig. 4b, the small roll-up of a heavy component (CH_4) was observed at the early stage of the breakthrough in Fig. 8a. It is caused by the displacement of the adsorbed CH_4 by the newly arrived CO through the pore. Therefore, the CO concentration in the gas phase steeply decreased, while that in the solid phase was relatively higher than the CH_4 concentration. At 400 sec in Fig. 8b, the concentration profiles of CO in the gas and solid phases were almost similar, whereas the profiles of CH_4 in both phases kept constant difference through the bed. In the case of a heavy component, a driving force of mass transfer was kept even at 1400 sec,

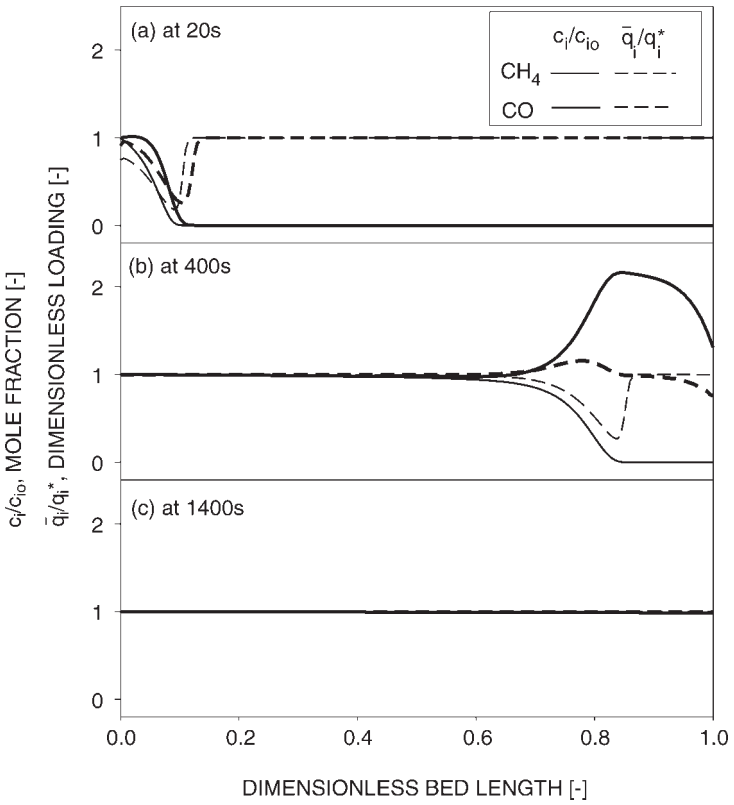

Figure 7. Bed profiles in the CMS bed, regenerated at 548 K, under 10 kg_f/cm^2 adsorption pressure and 6.8 LSTP/min feed rate at (a) 20 sec, (b) 400 sec, and (c) 1400 sec. (calculated by LDF model).

which was different from Fig. 7c. Also, since the diffusion of CH_4 into the CMS was very slow, its concentration on the solid phase was nearly the same through the bed. Moreover, the CH_4 concentration profile was increased very slowly with time, which seemed to be independent of the concentration in the gas phase.

To provide a clearer insight into the adsorption dynamics in the equilibrium and kinetic beds, the temperature profiles inside the beds are presented in Figs. 9 and 10. The adsorption process is intrinsically exothermic and the heat released during the adsorption makes the breakthrough nonisothermal. As the concentration wave fronts of CO and CH_4 propagate along the bed, the heat of adsorption brings temperature rise in the equilibrium control bed

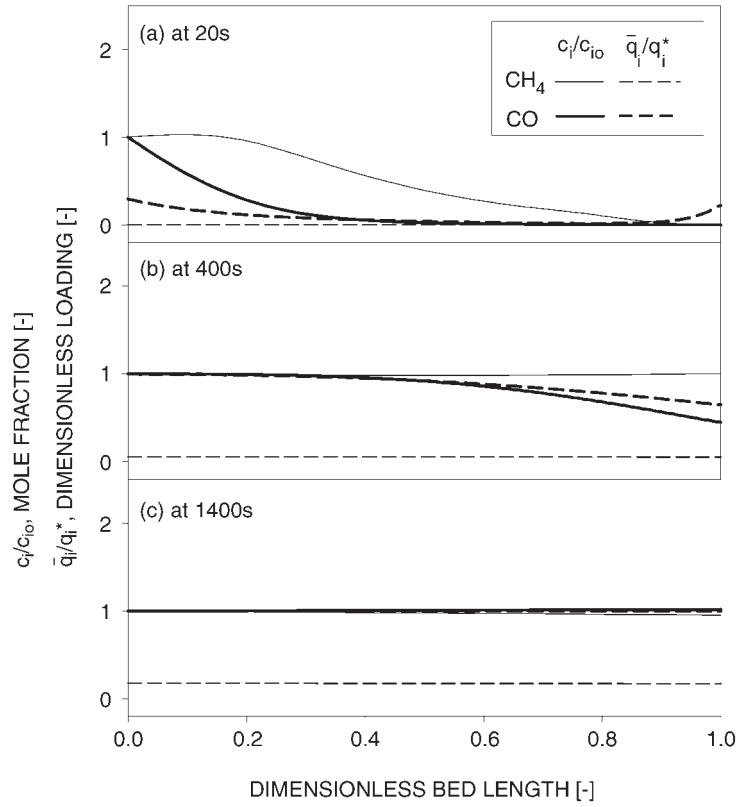

Figure 8. Bed profiles in the CMS bed, regenerated at 423 K, under 10 kg_f/cm^2 adsorption pressure and 6.8 LSTP/min feed rate at (a) 20 sec, (b) 400 sec, and (c) 1400 sec. (calculated by Darken–LF model).

in Fig. 9. Because the concentration wave fronts of CO and CH_4 are very close at the feed end in Fig. 7a, one temperature excursion is observed near the feed end in Fig. 9a. However, the temperature profile began to show a small inflection at around 200 sec. in Fig. 9b. Then, as concentration wave fronts of CO and CH_4 propagate along the bed, the separated two temperature excursions can be seen clearly in Figs. 9c and 9d. Since the wave velocity of CO is significantly different from that of CH_4 in Fig. 7b, temperature rose twice and temperature excursion peaks were highly separated along the bed. The first excursion of the temperature profile by the CO adsorption decreased slightly because of the heat transfer and desorption of CO by the CH_4 concentration

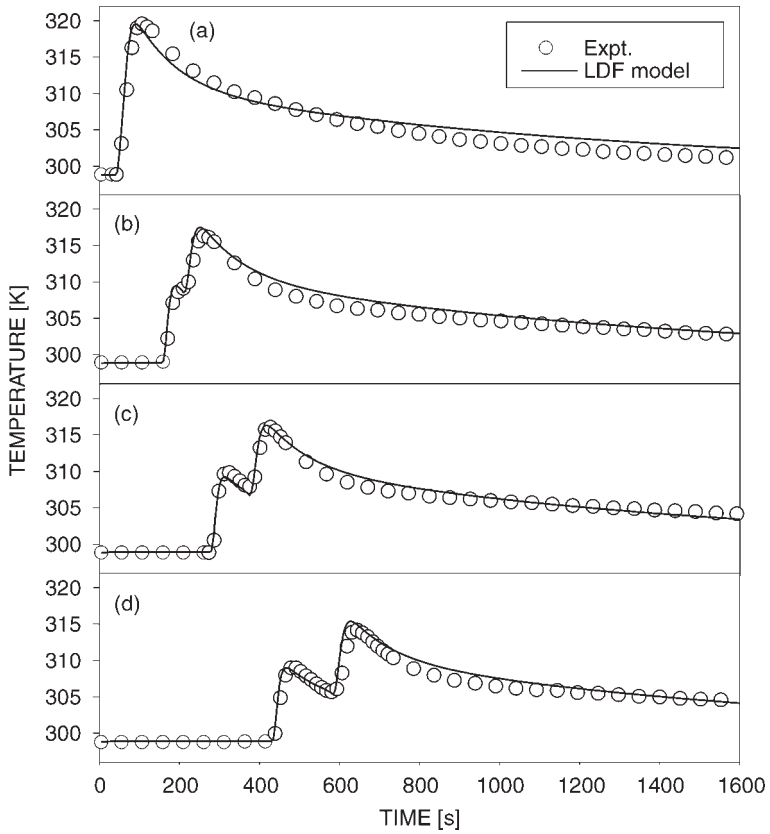

Figure 9. Temperature history at the position of (a) 10 cm, (b) 30 cm, (c) 50 cm, and (d) 75 cm from the feed end under 10 kg_f/cm^2 adsorption pressure and 6.8 LSTP/min feed rate in the CMS bed regenerated at 548 K.

wave front. Then, the latter temperature peak was caused by the adsorption of CH_4.

As shown in Fig. 10, the temperature profiles in the kinetically controlled bed were very different from those in the equilibrium controlled bed. The temperature increase by the adsorption was less than 3 K, which was near the isothermal condition. Compared with the equilibrium controlled CMS bed regenerated at 548 K, the average amount adsorbed of the heavy component is negligible, as shown in Fig. 8. As a result, the adsorption dynamics in the kinetically controlled CMS bed regenerated at 423 K were operated near the isothermal condition due to the very slow diffusion of the strong adsorbate (CH_4).

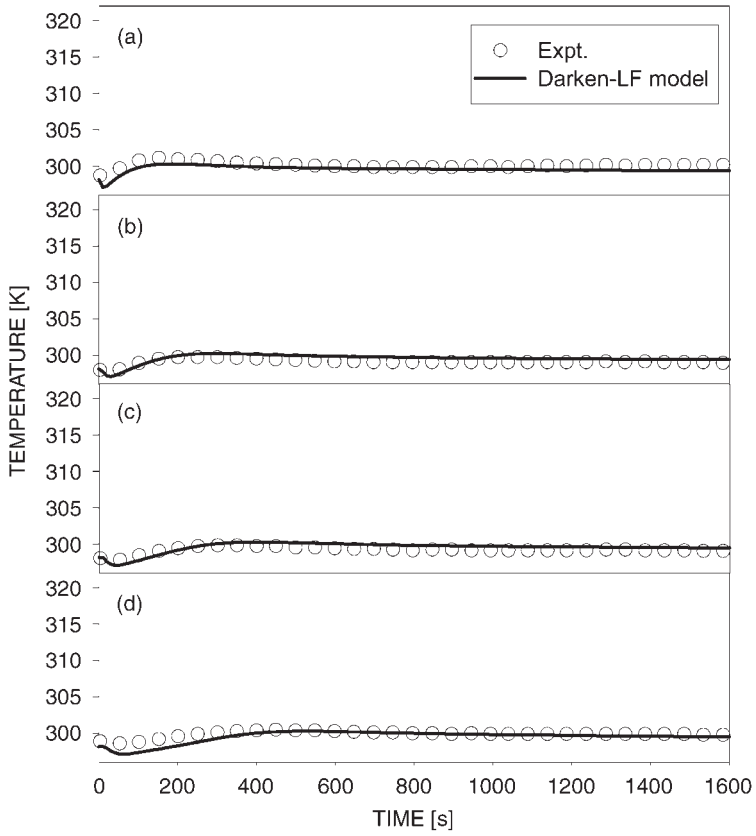

Figure 10. Temperature history at the position of (a) 10 cm, (b) 30 cm, (c) 50 cm, and (d) 75 cm from the feed end under 10 kg_f/cm^2 adsorption pressure and 6.8 LSTP/min feed rate in the CMS bed regenerated at 423 K.

CONCLUSION

The adsorption dynamics of a ternary hydrogen mixture in the CMS bed were compared experimentally and theoretically with fixed beds packed with activated carbon and zeolite 5A. The variation of the adsorption dynamics by the difference in the regeneration temperature of CMS also was investigated because it entirely changed the adsorption characteristics. In this study the CMS was regenerated at 423 K and 548 K.

In the CMS bed regenerated at high temperature, the kinetic effect became weak due to the pore enlargement of the CMS for regeneration. As

a result, separation was mainly accomplished by the equilibrium mechanism and the breakthrough behavior showed a typical roll-up of a light component in a multicomponent system. The overall behavior resembled that of the activated carbon bed. On the other hand, the breakthrough behavior of zeolite 5A bed was somewhat different since both wave fronts of CO and CH_4 proceeded almost simultaneously in the zeolite 5A bed.

In the CMS bed regenerated at low temperature, the breakthrough order of the components is interchanged and the breakthrough of a heavy component occurred almost immediately due to a much slower uptake of CH_4. At the experimental condition used in the work, the mean value of the diffusion constant of CO on the CMS regenerated at 423 K was about 1.2×10^2 times higher than that of CH_4. Because the adsorption dynamics totally depended on the kinetic effect, the developed rate model introducing the Darken model and a structural diffusion model was applied in the simulation. The variable diffusivity models that have the concentration dependent rate parameter showed better prediction than that by the constant diffusivity model.

Compared with the equilibrium controlled CMS bed regenerated at 548 K, the average adsorbed amount of the heavy component is negligible. As a result, the adsorption dynamics in the kinetically controlled CMS bed regenerated at 423 K were operated near the isothermal condition due to the very slow diffusion of the heavy component. The range of temperature variation was only about 3 K. Therefore, the CMS bed may be used for the recovery of H_2 and CH_4 simultaneously from the ternary system.

NOMENCLATURE

A_w	cross sectional area of the wall (cm^2)
B	equilibrium parameter for Langmuir–Freundlich model (atm^{-1})
$[B]$	matrix of inverted Maxwell–Stefan diffusivities (sec/cm^2)
C_i	i component concentration in bulk phase (mol/cm^3)
C_{pg}, C_{ps}, C_{pw}	gas, pellet, and wall heat capacity, respectively (cal/g K)
$[D]$	matrix of Fick diffusivities (cm^2/sec)
D_e	effective diffusivity defined by solid diffusion model (cm^2/sec)
$Đ_i$	Maxwell–Stefan diffusivity of component i (cm^2/sec)
D_o	diffusional time constants (cm^2/sec)
D_L	axial dispersion coefficient (cm^2/sec)
h_i	heat transfer coefficient at the inner wall ($cal/cm^2\,K\,sec$)

h_o	heat transfer coefficient at the outer wall (cal/cm^2 K sec)
$\cdot\bar{H}$	average heat of adsorption (cal/mol)
k	parameter for Langmuir–Freundlich model
K	proportionality parameter for LDF model (—)
K_L	axial thermal conductivity (cal/cm sec K)
L	bed length (cm)
n	equilibrium parameter for Langmuir–Freundlich model (—)
P	total pressure (atm)
q, q^*, $\bar{q}$	amount adsorbed, equilibrium amount adsorbed, and average amount adsorbed, respectively (mol/g)
q_m	equilibrium parameter for Langmuir–Freundlich model (mol/g)
R_p	radius of pellet (cm)
R_{Bi}, R_{Bo}	inside and outside radius of the bed, respectively (cm)
t	time (sec)
T_{atm}	temperature of atmosphere (K)
T, T_w	pellet or bed temperature and wall temperature, respectively (K)
u	interstitial velocity (cm/sec)
v	superficial velocity (cm/sec)
z	axial distance in bed from the inlet (cm)

Greek Symbols

δ_{ij}	Kronecker delta ($\delta_{ij} = 1$ for $i = j$, $\delta_{ij} = 0$ for $i \neq j$)
$[\Gamma]$	matrix of thermodynamic factors (—)
ε, ε_t	voidage of adsorbent bed and total void fraction, respectively (—)
θ	fractional surface occupancy (—)
ρ_g, ρ_p, ρ_B, ρ_w	gas density, pellet density, bulk density, and bed wall density, respectively (g/cm^3)
ω	LDF coefficient (sec^{-1})
μ	viscosity (g/cm sec)

Subscripts

B	bed
i	component i
p	pellet
g	gas phase

s	solid phase
V	vacant site
w	wall

ACKNOWLEDGMENTS

The financial support of the Korea Energy Management Corporation (2001-N-HY02-P-01) and LNG Technology Research Center in Korea Gas Co. are acknowledged gratefully.

REFERENCES

1. Ruthven, D.M. *Pressure Swing Adsorption*; VCH: New York, 1994.
2. Yang, R.T. *Gas Separation by Adsorption Processes*; Butterworths: Boston, 1987.
3. Chen, Y.D.; Yang, R.T.; Uawithya, P. Diffusion of oxygen, nitrogen and their mixtures in carbon molecular sieve. AIChE J. **1994**, *40* (4), 577–585.
4. Bae, Y.-S.; Lee, C.-H. Sorption kinetics of eight gases on a carbon molecular sieve at elevated pressure: Part I. Experimental. Carbon **2004**, in revision.
5. Kapoor, A.; Yang, R.T. Kinetic separation of methane-carbon dioxide mixture by adsorption on molecular sieve carbon. Chem. Eng. Sci. **1989**, *44* (8), 1723–1733.
6. Kikkinides, E.S.; Yang, R.T.; Cho, S.H. Concentration and recovery of CO_2 from flue gas by pressure swing adsorption. Ind. Eng. Chem. Res. **1993**, *32*, 2714–2720.
7. Sircar, S.; Kumar, R. Adiabatic adsorption of bulk binary gas mixtures. Ind. Eng. Chem. Process Des. Dev. **1983**, *22*, 271–280.
8. Sircar, S.; Kumar, R. Column dynamics for adsorption of bulk binary gas mixtures on activated carbon. Sep. Sci. Technol. **1986**, *21*, 919–939.
9. Hwang, K.S.; Jun, J.H.; Lee, W.K. Fixed-bed adsorption for bulk component system. Non-equilibrium, non-isothermal, and non-adiabatic model. Chem. Eng. Sci. **1995**, *50* (5), 813–825.
10. Silva, J.A.C.; Rodrigues, A.E. Fixed-bed adsorption of two linearly adsorbed components in presence of an inert. Chem. Eng. Sci. **1998**, *53* (20), 3513–3520.
11. Yang, J.; Lee, C.-H. Adsorption dynamics of a layered bed PSA for H_2 recovery from coke oven gas. AIChE J. **1998**, *44* (6), 1325–1334.

12. Farooq, S.; Ruthven, D.M. Dynamics of kinetically controlled binary adsorption in a fixed bed. AIChE J. **1991**, *37* (2), 299–301.
13. Park, J.-H.; Kim, J.-N.; Cho, S.-H.; Kim, J.-D.; Yang, R.T. Adsorber dynamics and optimal design of layered beds for multicomponent gas adsorption. Chem. Eng. Sci. **1998**, *53* (23), 3951–3963.
14. Ahn, H.; Chun, C.; Park, M.; Ahn, I.-S.; Lee, C.-H. Thermal effects on the breakthrough curve of a hydrogen ternary system at a fixed bed. Sep. Sci. Technol. **2001**, *36* (10), 2117–2141.
15. Gupta, R.; Farooq, S. *Numerical Simulation of Kinetically Controlled Bulk PSA Separation Process Based on a Bidisperse Pore Diffusion Model*, Proceedings of the 8th APCChE Congress, **1999**, *3*, 1753–1756.
16. PSE Ltd. *gPROMS Introductory User Guide*; Bridge Studios: London, 2002. Release 2.1.1
17. Jee, J.-G.; Kim, M.-B.; Lee, C.-H. Adsorption characteristics of hydrogen mixtures in a layered bed: binary, ternary, and five-component mixtures. Ind. Eng. Chem. Res. **2001**, *40* (3), 868–878.
18. Lee, C.-H.; Yang, J.; Ahn, H. Effect of carbon-to-zeolite ratio on layered bed H2 PSA for coke oven gas. AIChE J. **1999**, *45* (3), 535–545.
19. Doong, S.J.; Yang, R.T. Bulk separation of multicomponent gas mixtures by pressure swing adsorption: pore/Surface diffusion and equilibrium models. AIChE J. **1986**, *32* (3), 397–410.
20. Bird, R.B.; Stewart, W.E.; Lightfoot, E.N. *Transport Phenomena*; Wiley: New York, 1960.
21. Jee, J.-G.; Park, H.-J.; Haam, S.-J.; Lee, C.-H. Effects of nonisobaric and isobaric steps on O_2 PSA for aerator. Ind. Eng. Chem. Res. **2002**, *41* (17), 4383–4392.
22. Farooq, S.; Ruthven, D.M. Numerical simulation of a kinetically controlled pressure swing adsorption bulk separation process based on a diffusion model. Chem. Eng. Sci. **1991**, *46* (9), 2213–2224.
23. Farooq, S.; Rathor, M.N.; Hidajat, K. A. Predictive model for a kinetically controlled pressure swing adsorption separation process. Chem. Eng. Sci. **1993**, *48* (24), 4129–4141.
24. Krishna, R.; Wesselingh, J.A. The Maxwell-Stefan approach to mass transfer. Chem. Eng. Sci. **1997**, *52* (16), 861–911.
25. Van Den Broeke, L.J.P.; Krishna, R. Experimental verification of the Maxwell-Stefan theory for micropore diffusion. Chem. Eng. Sci. **1995**, *50* (16), 2507–2522.
26. Krishna, R. Multicomponent surface diffusion of adsorbed species: a description based on the generalized maxwell-stefan equations. Chem. Eng. Sci. **1990**, *45* (7), 1779–1791.
27. Ackley, M.W.; Yang, R.T. Kinetic separation by pressure swing adsorption: method of characteristics model. AIChE J. **1990**, *36* (8), 1229–1238.

28. Do, D.D. A model for surface diffusion of ethane and propane in activated carbon. Chem. Eng. Sci. **1996**, *51* (17), 4145–4158.
29. Bae, Y.-S. Study on the Sorption Equilibrium and Kinetics of Seven Pure Gases on CMS. Yonsei University: Korea, 2001; M. Eng. Thesis.
30. Bae, Y.-S.; Kim, K.-I.; Lee, C.-H. *Comparison of Adsorption Equilibrium and Kinetics of Seven Pure Gases in a Carbon Molecular Sieve*, Proceedings of Separation Technology, **2001**, *2*, 678–682.